OPEN

NPG Asia Materials (2016) 8, e278; doi:10.1038/am.2016.72
www.nature.com/am

ORIGINAL ARTICLE

Deep blue energy harvest photovoltaic switching by heptazole-based organic Schottky diode circuits

Junyeong Lee[1,3], Syed Raza Ali Raza[1,2,3], Pyo Jin Jeon[1], Jin Sung Kim[1] and Seongil Im[1]

We report novel photovoltaic (PV) switching based on the low exciton-binding energy property of an organic heptazole ($C_{26}H_{16}N_2$) thin film after fabrication of an heptazole-based Schottky diode. The Schottky diode cell displayed an instantaneous voltage of 0.3 V as an open circuit voltage (V_{OC}) owing to the work function difference between the Schottky and ohmic electrode under deep blue illumination. Four tandem diode cells therefore produced ~ 1.2 V. As a PV diode circuit can be formed using an even number of diodes, a photo-excited charge accumulation takes place, generating V_{OC} in the central electrode of the tandem diode array by illuminating one half of the array. An electron–hole recombination then also takes place in that electrode by illuminating the other half, making the V_{OC} decrease to 0 V. Utilizing this charge accumulation and recombination under deep blue illumination, we successfully demonstrated quite fast PV optical switching, logic gating and, ultimately, the gate switching of an organic field-effect transistor. We therefore concluded that our self-powered PV-induced switching was novel and promising enough to open a new door for energy harvest-related device applications in organics.
NPG Asia Materials (2016) **8,** e278; doi:10.1038/am.2016.72; published online 10 June 2016

INTRODUCTION

Photovoltaic (PV) effects have long been studied for their main applications in solar energy and PV cells, which are energy-harvesting devices.[1–6] Organic and inorganic semiconductors have been used as active components of those energy-harvesting devices in a variety of diode forms, including Schottky diodes,[7–10] p-n diodes[11–14] and p-i-n diodes,[15–18] showing outstanding progress in enhancing their power efficiencies.[19,20] This study reports a rather different new application, dynamic PV switching and voltage generation by deep blue photons. Dynamic PV switching has so far been ignored in organic electronics and rarely attempted in inorganics despite its potential great usefulness as a dynamic energy-harvesting method.[13,21–25] In fact, dynamic PV switching has only been reported for its limited practical applications with inorganic nanostructure junctions, as seen in Supplementary Table S1.[13,21–25] Simply speaking, instantaneously built-in voltage can be used as a switching signal induced by energetic photons (ON/OFF: photo-induced charge collection/recombination), as any semiconductor thin film possesses electrodes for charge collection and recombination within a diode array. This type of self-powered voltage generation can have various applications, including ultraviolet (UV) and visible light detection, biological and chemical study in a wireless health-care platform, powerless communications and so on.[26] Particularly, selective detection and absorption of deep blue and UV photons without any aid of electric power would be very important for eye protection applications in these days.[27]

The present study on PV switching and photo-induced dynamic energy harvesting used an organic semiconductor-based Schottky diode, as it is low cost and easy to fabricate on a glass or plastic substrate. Our organic PV switching diodes could be integrated into a tandem device array on a large area substrate to produce higher photo-voltage, which cannot yet be performed with inorganic nano-dimension diodes. The PV switching and voltage generation mechanisms are explained in detail. The most important property of the organic semiconductor thin film is its exciton-binding energy, which needs to be as small as possible for the easy/fast charge dissociation of photo-excited excitons and superior energy harvesting. In this context, we chose an heptazole ($C_{26}H_{16}N_2$) thin film, as the latter showed a rather small exciton-binding energy of ~ 40 meV, while pentacene ($C_{22}H_{14}$) and dinaphtho[2,3-b:2′,3′-f]thieno[3,2-B]thiophene (DNTT; $C_{22}H_{12}S_2$) revealed somewhat larger binding energies of 100 and 120 meV, respectively. (See Supplementary Figure S1 and Supplementary Table S2 for a detailed comparison of the respective exciton-binding energy properties of heptazole, DNTT[28] and pentacene thin films based on photo-excited charge collection spectroscopic results.[29]) Besides its small exciton-binding energy, our organic heptazole with 2.95 eV energy band gap sensitively and selectively detects deep blue/UV photons in PV switching operations, which would be promising toward smart eye protection glass applications.[27] Because of the intrinsic potential energy (or work function) difference between Al and indium-tin-oxide (ITO), our Schottky diode displayed an instantaneous voltage of 0.3 V by deep blue illumination from a laser diode, and four tandem diode cells could therefore produce ~ 1.2 V when integrated onto the same glass substrate. Using several diode circuitries, we demonstrate 50-ms short PV optical switching,

[1]Institute of Physics and Applied Physics, Yonsei University, Seoul, Korea and [2]Department of Physics, University of Azad Jammu and Kashmir, Muzaffarabad, Pakistan
[3]These authors contributed equally to this work.
Correspondence: Professor S Im, Institute of Physics and Applied Physics, Yonsei University 50 Yonsei-ro, Science Building #240, Seodaemun-gu, Seoul 120-749, Korea.
E-mail: semicon@yonsei.ac.kr
Received 19 August 2015; revised 14 March 2016; accepted 22 March 2016

logic gating and, ultimately, the gate switching of an organic field-effect transistor (FET).

EXPERIMENTAL PROCEDURES

Fabrication of organic Schottky diode

A glass substrate was first cleaned with acetone, methanol and deionized water for 5 min each. A transparent ITO electrode was deposited onto the cleaned substrate using a DC sputtering system. Organic heptazole (Luminano Co., Seoul, Korea) and pentacene (Sigma Aldrich Co., St Louis, MO, USA) semiconductors were carefully grown onto the ITO electrode with an organic molecule beam deposition system, followed by Al Schottky electrode deposition using a thermal evaporation system. Every electrode and semiconductor layer was 50-nm thick and patterned with a conventional shadow mask. Finally, the device-to-device interconnection of Ti/Au was patterned with a DC sputtering system.

Fabrication of organic FET

An Al gate electrode was deposited on a precleaned glass substrate with a thermal evaporator. A 50-nm-thick Al_2O_3 gate insulator layer was then grown with an atomic layer deposition system using a trimethylaluminum precursor and water vapor reactant as usual. As the surface of the Al_2O_3 insulator was hydrophilic, the hydrophobic polymer of CYTOP (Asahi Glass Co., Tokyo, Japan) was coated and annealed in an oven at 180 °C for 2 h. Afterward, the heptazole small molecule was carefully grown again by organic molecule beam deposition with a deposition rate of 0.1 nm s^{-1}, followed by Au source/drain electrodes with a thermal evaporation system. Every electrode and semiconductor layer was 50-nm thick and patterned with a conventional shadow mask.

Electrical and photoelectrical measurement

The static electrical behaviors of the Schottky diode and the FET were characterized using a semiconductor parameter analyzer (HP 4155C, Agilent Technologies, Santa Clara, CA, USA). The electrical dynamics measurements were investigated with a function generator (AFG 310, Sony, Tokyo, Japan/Tektronix Inc., Beaverton, OR, USA) and an oscilloscope (TDS210, Tektronix). The photoelectric measurements were taken by laser diodes with different wavelengths: red (656 nm), green (531 nm), and blue (406 nm). Their optical power density was 4, 2 and 1.5 mW cm^{-2} for the red, green and blue photons, respectively.

RESULTS AND DISCUSSION

We prepared all devices on a glass substrate. Figures 1a and b, respectively, display the cross-section schematics and plan-view optical image of our heptazole film-based Schottky diode, while Figure 1c shows the diode circuit made up of two diodes along with a real circuit image. In the Figure 1c circuits, L1 and L2 represent same-intensity blue lights (406 nm laser diode, ~1.4 mW cm^{-2}) as separately illuminated onto each Schottky diode. Figure 1d shows dark and photo-induced current plots as a function of the applied voltage (V_a) obtained from the single diode of Figure 1b on both linear and log scales. The energy of the blue illumination was slightly higher than the band gap (~2.95 eV) of the crystalline heptazole film (a single heptazole molecule is shown in the inset).[30] (We also conducted spectral responsivity measurements with the same diode in a UV/visible range as illustrated in Supplementary Figures S2a–d, where the unique light selectivity for photo detection is confirmed at 2.95 eV or 410 nm with a responsivity of 15–35 mA W^{-1}). According to Figure 1d, an open circuit voltage (V_{OC}) of ~0.3 V was achieved along with a good photo-induced current of 100 nA (at a reverse bias voltage of −2 V) under the blue light, while after illumination (turn off), the current–voltage (*I–V*) curve went back to its dark state behavior. The ideality factor was ~2.3 and the ON/OFF current ratio was ~10^5. A more interesting *I–V* curve behavior achieved from the circuit configuration of Figure 1c under the blue L1 and L2 combination can be observed in Figure 1e (for more precise V_{OC} information, the corresponding *I–V* curves are provided on a linear scale in

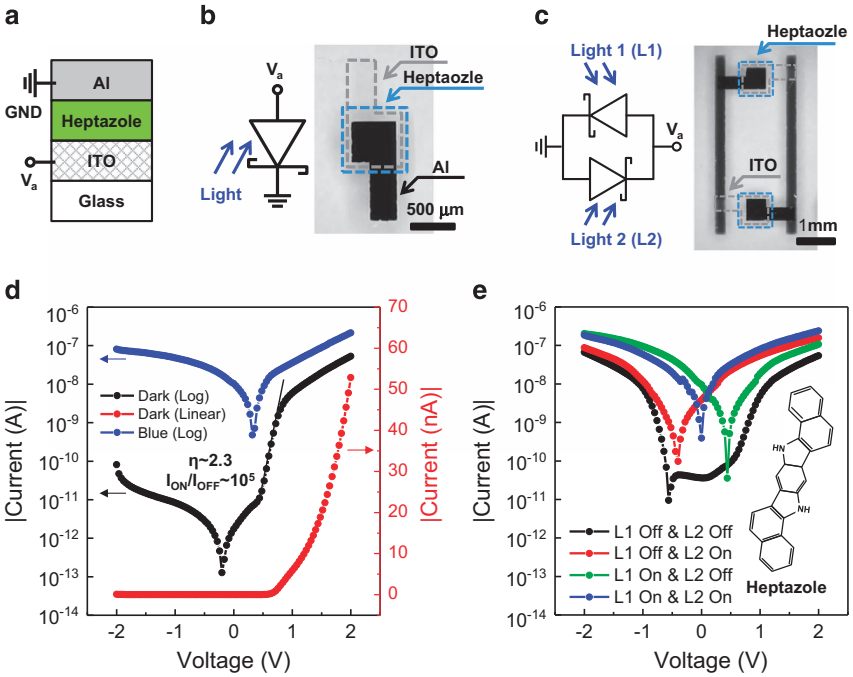

Figure 1 (**a**) Cross-section schematic and (**b**) optical image of our heptazole-based Schottky diode with circuit configuration. (**c**) Schematic circuit diagram and optical image for the circuit composed of two heptazole Schottky diodes (Blue and gray dashed lines in optical images indicate patterned heptazole semiconductor and ITO electrode, respectively.). *I–V* curves under dark and blue illumination for (**d**) single diode (inset: heptazole molecule structure) and (**e**) double diode circuit. L1 and L2 are representing the Light 1 on upper diode and Light 2 on downside diode, respectively, as shown in (**c**).

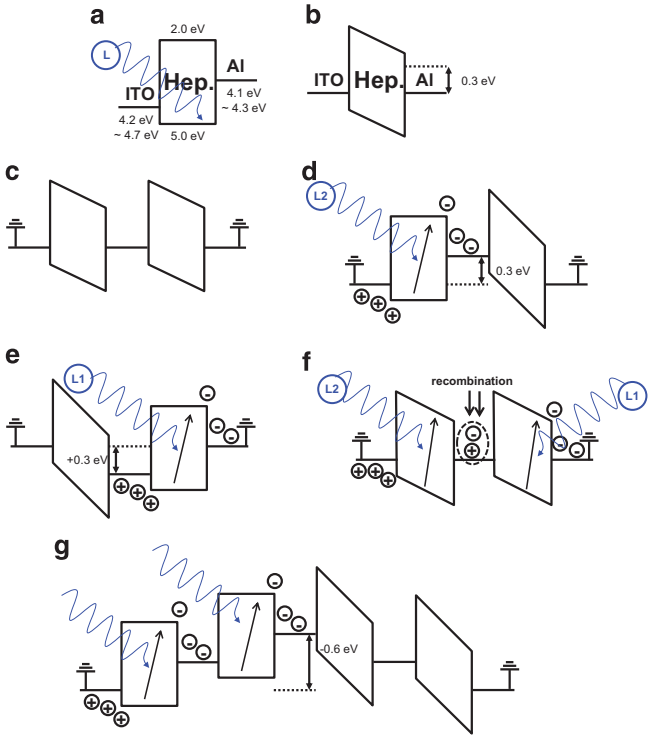

Figure 2 The band diagrams of a single diode (**a**) after and (**b**) before illumination (L). The band diagrams of two diode PV circuit (**c**) in the dark, under (**d**) left diode-illuminating (L1-off/L2-on), (**e**) right diode-illuminating (L1-on/L2-off) and (**f**) simultaneous illuminating (L1-on/L2-on). Each band diagram explains how V_{OUT} signal is generated. (**g**) The band diagram of multiple (tandem) diode PV circuit produces a large V_{OUT} of 0.6 V.

Supplementary Figures S3a and b). In the dark, the *I–V* curve appeared quite symmetric as the diode circuit behavior should always be forward biased: the current passes through the upper diode under (+) V_a but chooses the down-side one under (−) V_a. When L1 was off and L2 was on, a V_{OC} of −0.3 V was obtained, while a V_{OC} of 0.3 V was obtained in L1 on/L2 off conditions (this case was almost the same as in Figure 1d). However, when both L1 and L2 were on, the V_{OC} reverted to 0 V and the *I–V* curve appeared symmetric with a large photocurrent. In this Schottky diode circuit, the behavior and size of the V_{OC} were important as the V_{OC} eventually turns into an instantaneous output voltage (V_{OUT}) signal under dynamic illuminations, which means that the V_{OUT} in the PV circuits can be extracted by optical switching (or illuminating photons onto spatially separated diodes).

For more detailed explanations, the energy band models of the two-diode circuit are presented in Figures 2a–g. Figure 2a shows the detailed energy-level information of the organic heptazole film, Al and ITO, allowing us to calculate a Schottky barrier height of 0.92 eV from the band diagram (this number was confirmed by the temperature-dependent *I–V* measurements presented in Supplementary Figures S4a and b). According to the band diagrams for a single diode in Figures 2a and b, the 0.3 V V_{OC} originated from the work function difference between the ITO and Al (Schottky) electrodes:[31,32] when the blue light illuminated the heptazole thin film through the glass substrate, the electron charges moved to Al and the hole charges migrated to the ITO side until the heptazole band became flat. We then extended the single-diode band diagram to a double-diode band model, as shown in Figures 2c–f, which, respectively, picture dark, left diode-illuminating (L2), right diode-illuminating (L1) and simultaneous illuminating (L1, L2) situations. Figures 2d and e explain the way the two-diode PV circuit could gain a V_{OUT} of 0.3 V and −0.3 V, respectively, while Figure 2f illustrates why our diode circuit reverted to a V_{OUT} of 0 V. Figure 2f simply describes the recombination of the photo-induced electrons and holes in the midpoint (the connection electrode) between the two diodes so that the point had zero potential. This explained the photo-induced *I–V* curve behavior shown in Figures 1d and e comprehensively. Moreover, the phenomena could be applied to increase the V_{OUT} or V_{OC} by using multiple (tandem) diode PV circuits as shown schematically in Figure 2g, where four diodes connected in series produced a twice-larger V_{OUT} of 0.6 V under light conditions.

Based on the above understandings, we measured the dynamic PV switching in a single-diode and a two-diode circuit. According to the time-domain V_{OUT} plot of the single-diode circuit in Figure 3a, >0.3 V were repeatedly obtained under periodic blue illumination conditions, although the V_{OUT} did not decrease to 0 V but almost stopped near 0.2 V. A similar phenomenon was observed in the two-diode circuit of Figure 3b, where L1 was periodically on while L2 stayed off all along. This slow switching-off behavior in the single diode was attributed to the long stay of floated hole charges (or slow discharge) in the ITO. This long stay was presumed to be caused by the hole barrier at the interface between the heptazole film and the ITO (Figure 2a). In the two-diode circuit, a long hole stay again occurred at the point between the two diodes, as evidenced by Figure 2e. Figure 3c displays the way to shorten the charge stay: this can be carried out by applying a short L2 pulse immediately after turning off L1. According to Figure 3c, the V_{OUT} dropped closer to 0 V as the L2 pulse time grew longer. A 10-ms short L2 pulse seemed not to make a visible difference from the previous case (Figure 3b), while a 50-ms long L2 pulse achieved a very good V_{OUT} drop without delay. In view of the band diagram of Figure 2f, the fast switch-off was easy to understand: the floated holes in the middle of the circuit rapidly recombined with the photo-electrons injected by the L2 pulse. When the L2 illumination time was long enough with L1 off, the photo-electrons were accumulated in the location between the two diodes even after recombination, eventually producing a (−) V_{OUT} as observed in Figure 3d (which corresponds to the band model of Figure 2d). In addition, according to Figure 3e, if the L1 was always on, the periodic illumination of L2 could enable the circuit to repeat a (+) and 0 V V_{OUT} through repeated turn-off (Figure 2e) and turn-on (Figure 2f), respectively. We therefore defined the phenomenon presented in Figure 3d as optical switching and that shown in Figure 3e as optical inversion. Figure 3f contains the example photos obtained during the PV circuit operations illustrated in Figure 3d (optical switching) and Figure 3e (optical inversion: NOT gating); the real-time records for those operations are provided in Supplementary Video File.

In fact, PV optical switching could be directly applied to gate switching in a real organic FET, which also uses a heptazole thin film on glass as its active channel. Figure 4a shows a schematic device cross-section of our organic FET with a 30-nm CYTOP/50-nm atomic layer-deposited Al_2O_3 bilayer gate dielectric, while Figure 4c displays the drain current–gate voltage (I_D–V_{GS}) transfer curves of the FET.[33] Figure 4b shows optical plan-view images of the two-diode FET circuit connected by an Al wire. Here a constant drain voltage (V_{DS} = −1 V) was supplied to the FET, although its gating was operated by the optically switched V_{OUT} signal of the PV diode circuit. Those PV-induced gatings are pictured in Figures 5a–i, where the PV-induced V_{OUT} now works as a V_{GS}. For instance, the first two-diode circuit of Figure 5a produced −0.3 and 0.3 V by periodic PV

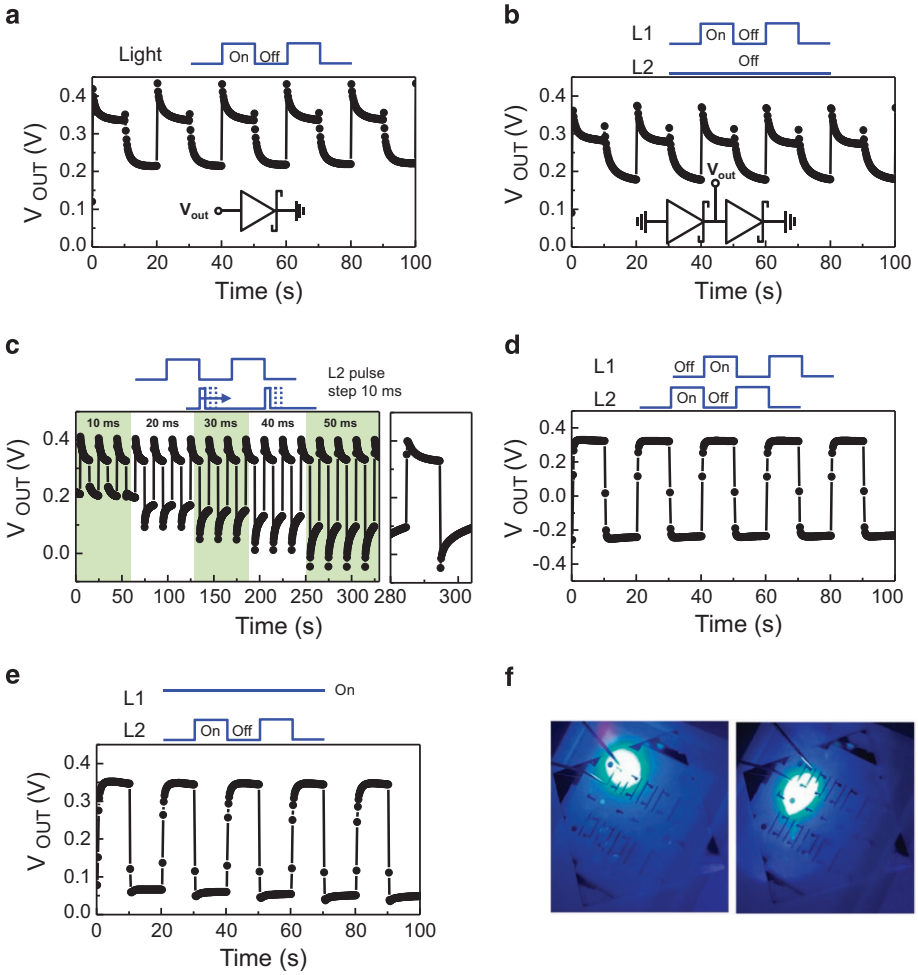

Figure 3 Time domain V_{OUT} plot obtained under periodic blue illuminations for (**a**) single diode and (**b**) two diode PV circuits. (Each inset shows schematic diode circuits.) The time domain V_{OUT} plots obtained from two diode circuit with (**c**) short L2 pulse (ranging from 10 to 50 ms) after turning off L1, (**d**) alternate L1/L2 illuminations for optical switching phenomenon and (**e**) periodic L2 illumination for optical inversion (L1 always turns on during this operation). (**f**) Optical images of PV circuit operations for switching and inversion. (Watch Supplementary Video for more details.)

switching, as shown in the time-domain V_{OUT} plot of Figure 5b. However, this input or gate voltage then modulated the I_D from 0 to -0.7 nA on a linear scale (Figure 5c). The I_D modulation became larger when multiplying the diode number in tandem mode: the second four-diode circuit of Figure 5d produced a V_{OUT} and I_D of -0.6 V and -1.4 nA, respectively (as seen in Figures 5e and f), while another circuit with eight diodes produced -1.2 V and ~ -3.0 nA (as observed in Figures 5g–i). PV optical switching was again noted in a pentacene($C_{22}H_{14}$)-based Schottky diode circuit with the same electrodes (Al and ITO), as shown in Supplementary Figures S5 and S6. According to Supplementary Figure S6, PV-induced optical inverting and switching visibly occurred even under red laser light (1.5 mW cm^{-2}), as the energy gap of pentacene film is known to be 1.97 eV (photoelectric gap) or 1.85 eV (optical gap).[34] However, the switching speed appeared to be one order of magnitude lower than that of the heptazole-based Schottky diode (fall/rise time $\sim$0.5 s), although the switching speed improved under blue light (but remained slower than that of the heptazole device). The speed difference was believed to result from the different exciton-binding energies of the crystalline heptazole and pentacene films (40 vs 120 meV, respectively).[29,30,34] As the recombination of the holes and electrons takes place within the electrode between the two organic diodes, efficient separation of the photo-excited charges or dissociation of the excitons in the semiconductor layer is required. Although the heptazole device must present advantages over other devices with a larger exciton-binding energy in terms of switching speed, PV-induced switching was in any case proven to be a working process. On the one hand, our organic semiconductor still had larger exciton-binding energy than its inorganic counterparts. Moreover, our organics had many traps/defects and grain boundaries causing low mobility, while most inorganic semiconductors are single crystalline. We believe that those aspects of exciton binding and defects/traps in organic semiconductors are key controlling elements of the response time delay, making it longer than those of inorganic ones (see Supplementary Table S1).[21–26]

As an additional experiment, we attempted to extend our diode circuit applications to OR and AND gate logic switching, as the optical inverting (NOT gating) in Figure 3e appeared successful. To study the OR and AND functions, we modified the circuits as shown in Figures 6a and b, using a 56-MΩ external resistor to rapidly discharge any accumulated carriers. In the case of the OR gate using a parallel diode circuit, the hole charges easily accumulated into the V_{OUT} terminal under the blue light on both diodes for a (1,1) signal. Even when the light illuminated only one of the two diodes, the hole

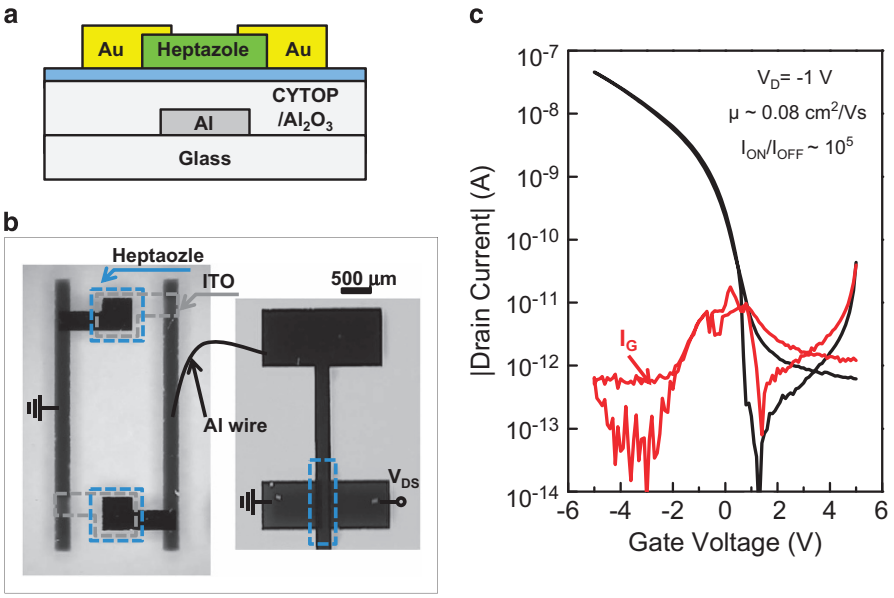

Figure 4 (**a**) Schematic device cross-section of heptazole-based field effect transistor. (**b**) Optical images of our heptazole-based Schottky diode–transistor circuit. Blue and gray dashed lines in optical images indicate heptazole semiconductor and ITO electrode, respectively, while black curved line represents Al wire connection for transistor gating. (**c**) Transfer characteristics of heptazole-based field effect transistor.

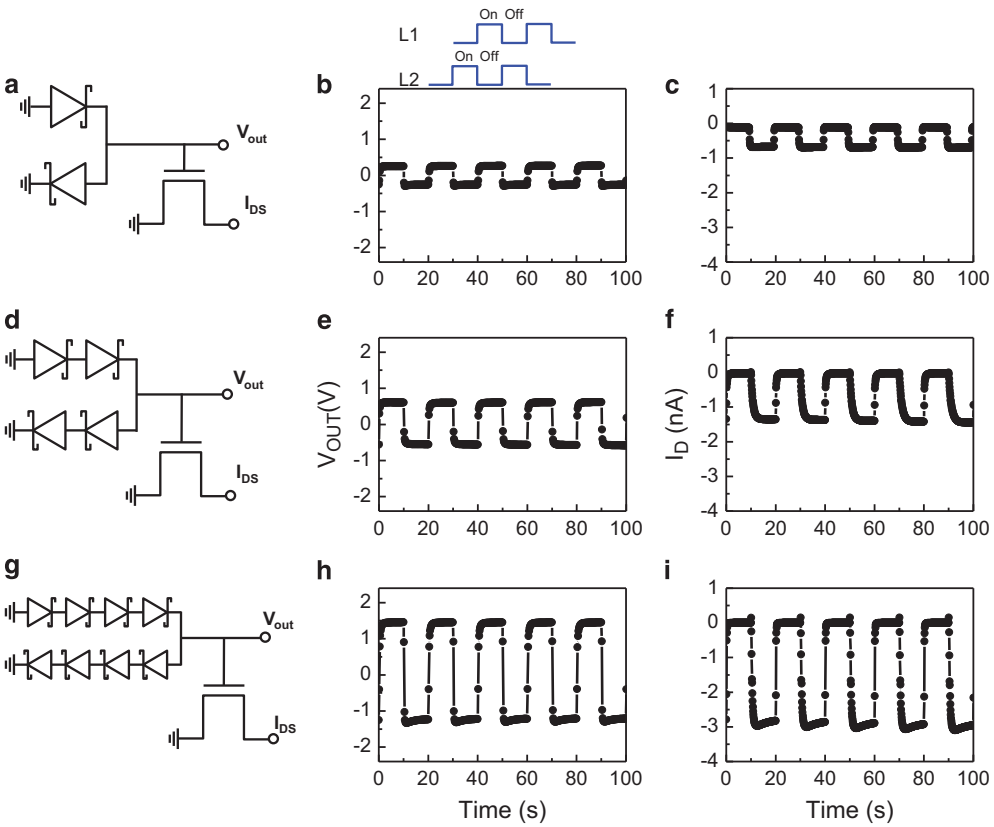

Figure 5 (**a**) Schematic circuit diagram of the PV-induced transistor gating. Time domain (**b**) PV-induced V_{OUT} plot from Schottky diode circuit and (**c**) I_D plot obtained from the PV-induced gate voltage modulation. Tandem mode circuit diagrams composed of (**d**) four diodes and (**g**) eight diodes are also shown, and as a result, respective V_{OUT} dynamics are demonstrated in panels (**e**) and (**h**) for transistor gating, which leads to I_D dynamics in panels (**f**) and (**i**).

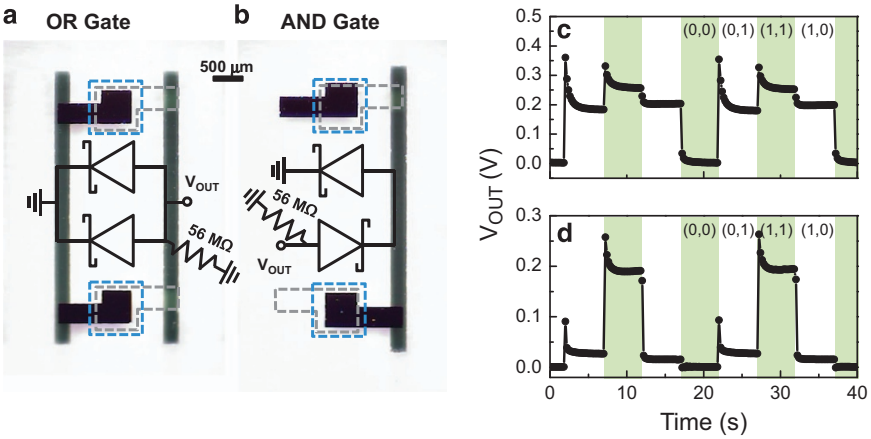

Figure 6 Schematic circuit diagrams and optical images of PV logic gates for (**a**) OR and (**b**) AND functions. A 56-MΩ external resistor is connected to rapidly discharge any accumulated carriers. Time domain V_{OUT} plots for respective logic gates are also shown in panels (**c**) and (**d**) for OR and AND.

accumulation was still effective for a (0,1) or (1,0) signal. An issue was to discharge those hole charges for a (0,0) signal. However, this problem could be effectively resolved by using an external resistor. Figure 6c presents the time-domain plot of the OR gate operation. Using a similar principle in a series circuit, we obtained the AND gate operation shown in Figure 6d. Likewise, our PV-induced diode circuits with the heptazole film could achieve all the basic logic functions of NOT, OR and AND under blue light without using any electric power.

CONCLUSION

In conclusion, we fabricated an organic heptazole-based Schottky diode and related diode circuits for PV-induced switching applications, which are a kind of energy-harvesting device from blue illumination. The Schottky diode cell displayed an instantaneous voltage of 0.3 V as its V_{OC} owing to the work function difference between two electrodes under blue illumination, and four tandem diode cells therefore produced ~1.2 V. As the photo-excited charges were accumulated into the central electrode of the diode array by illuminating the diodes in one half of the circuit, the V_{OC} turned into photo-induced V_{OUT}. Electron–hole recombination also took place within that electrode by illuminating the other half, thereby rapidly changing the V_{OUT} to 0 V. Further illumination even changed the polarity of the V_{OUT}. Based on those PV effects using an heptazole thin film with small exciton-binding energy, this study successfully demonstrated quite fast PV optical switching, logic gating and, ultimately, the gate switching of an organic FET. We therefore concluded that our self-powered PV-induced switching was novel and promising enough to open a new door for energy harvest-related device applications.

CONFLICT OF INTEREST

The authors declare no conflict of interest.

ACKNOWLEDGEMENTS

This research was supported by Nano Material Technology Development Program (Grant no. 2012M3A7B4049801), NRL Program (NRF-2014R1A2A1A01004815) and BK 21 plus through the National Research Foundation of Korea (NRF) funded by the Ministry of Science, ICT and Future Planning.

1 Chopra, K. L., Paulson, P. D. & Dutta, V. Thin-film solar cells: an overview. *Prog. Photovoltaics* **12**, 69–92 (2004).
2 Habas, S. E., Platt, H. A. S., van Hest, M. F. A. M. & Ginley, D. S. Low-cost inorganic solar cells: from ink to printed device. *Chem. Rev.* **110**, 6571–6594 (2010).
3 Li, G., Zhu, R. & Yang, Y. Polymer solar cells. *Nat. Photonics* **6**, 153–161 (2012).
4 Avrutin, V., Izyumskaya, N. & Morkoç, H. Semiconductor solar cells: recent progress in terrestrial applications. *Superlattices Microstruct* **49**, 337–364 (2011).
5 Heeger, A. J. Bulk heterojunction solar cells: understanding the mechanism of operation. *Adv. Mater.* **26**, 10–28 (2014).
6 Li, Y. Molecular design of photovoltaic materials for polymer solar cells: toward suitable electronic energy levels and broad absorption. *Acc. Chem. Res.* **45**, 723–733 (2012).
7 Yang, B., Guo, F., Yuan, Y., Xiao, Z., Lu, Y., Dong, Q. & Huang, J. Solution-processed fullerene-based organic Schottky junction devices for large-open-circuit-voltage organic solar cells. *Adv. Mater.* **25**, 572–577 (2013).
8 Li, X., Zhu, H., Wang, K., Cao, A., Wei, J., Li, C., Jia, Y, Li, Z, Li, X & Wu, D. Graphene-on-silicon Schottky junction solar cells. *Adv. Mater.* **22**, 2743–2748 (2010).
9 Karak, S., Lim, J. A., Ferdous, S., Duzhko, V. V. & Briseno, A. L. Photovoltaic effect at the Schottky interface with organic single crystal rubrene. *Adv. Funct. Mater.* **24**, 1039–1046 (2013).
10 Lee, J., Mubeen, S., Hernandez-Sosa, G., Sun, Y., Toma, F. M., Stucky, G. D. & Moskovits, M. High-efficiency panchromatic hybrid Schottky solar cells. *Adv. Mater.* **25**, 256–260 (2013).
11 Pospischil, A., Furchi, M. M. & Mueller, T. Solar-energy conversion and light emission in an atomic monolayer p–n diode. *Nat. Nanotechnol.* **9**, 257–261 (2014).
12 Jampana, B. R., Melton, A. G., Jamil, M., Faleev, N. N., Opila, R. L., Ferguson, I. T. & Honsberg, C. B. Design and realization of wide-band-gap (≈2.67 eV) InGaN p-n junction solar cell. *IEEE Electron Device Lett.* **31**, 32–34 (2010).
13 Cho, H. D., Zakirov, A. S., Yuldashev, S. U., Ahn, C. W., Yeo, Y. K. & Kang, T. W. Photovoltaic device on a single ZnO nanowire p–n homojunction. *Nanotechnology* **23**, 115401 (2012).
14 Bartelt, J. A., Douglas, J. D., Mateker, W. R., Labban, A. E., Tassone, C. J., Toney, M. F., Fréchet, J. M. J., Beaujuge, P. M. & McGehee, M. D. Controlling solution-phase polymer aggregation with molecular weight and solvent additives to optimize polymer-fullerene bulk heterojunction solar cells. *Adv. Energy Mater.* **4**, 1301733 (2014).
15 Park, S. H., Shin, I., Kim, K. H., Street, R., Roy, A. & Heeger, A. J. Tandem solar cells made from amorphous silicon and polymer bulk heterojunction sub-cells. *Adv. Mater.* **27**, 298–302 (2015).
16 Yoo, J., Nguyen, B., Campbell, I. H., Dayeh, S. A., Schuele, P., Evans, D. & Picraux, S. T. Si radial p-i-n junction photovoltaic arrays with built-in light concentrators. *ACS Nano.* **9**, 5154–5163 (2015).
17 Li, H., Yang, P., Chiou, S., Liu, H. & Cheng, H. A novel coaxial-structured amorphous-silicon p-i-n solar cell with Al-doped ZnO nanowires. *IEEE Electron Device Lett.* **32**, 928–930 (2011).
18 Crupi, I., Ruggeri, F. S., Grasso, A., Ruffino, F., Catania, G., Piro, A. M., Di Marco, S., Mirabella, S., Simone, F. & Priolo, F. Influence of the electro-optical properties of an α-Si:H single layer on the performances of a pin solar cell. *Thin Solid Films* **520**, 4036–4040 (2012).
19 Green, M. A., Emery, K., Hishikawa, Y., Warta, W. & Dunlop, E. D. Solar cell efficiency tables (Version 45). *Prog. Photovoltaics* **23**, 1–9 (2015).
20 You, J., Dou, L., Yoshimura, K., Kato, T., Ohya, K., Moriarty, T., Emery, K., Chen, C. C., Gao, J., Li, G. & Yang, Y. A polymer tandem solar cell with 10.6% power conversion efficiency. *Nat. Commun.* **4**, 1–10 (2013).

21 Xiang, D., Han, C., Hu, Z., Lei, B., Liu, Y., Wang, L., Hu, W. P. & Chen, W. Surface transfer doping-induced, high-performance graphene/silicon Schottky junction-based, self-powered photodetector. *Small* **11**, 4829–4836 (2015).
22 Hao, L. Z., Gao, W., Liu, Y. J., Liu, Y. M., Han, Z. D., Xue, Q. Z. & Zhu, J. Self-powered broadband, high-detectivity and ultrafast photodetectors based on Pd-MoS_2/Si heterojunctions. *Phys. Chem. Chem. Phys.* **18**, 1131–1139 (2016).
23 Kim, Y. L., Jung, H. Y., Park, S., Li, B., Liu, F., Hao, J., Kwan, Y.-K., Jung, Y. J. & Kar, S. Voltage-switchable photocurrents in single-walled carbon nanotube–silicon junctions for analog and digital optoelectronics. *Nat. Photonics* **8**, 239–243 (2014).
24 Hong, Q., Cao, Y., Xu, J., Lu, H., He, J. & Sun, J. Self-powered ultrafast broadband photodetector based on p–n heterojunctions of CuO/Si nanowire array. *ACS Appl. Mater. Interfaces* **6**, 20887–20894 (2014).
25 Bie, Y., Liao, Z., Zhang, H., Li, G., Ye, Y., Zhou, Y., Xu, J, Qin, Z. X., Dai, L & Yu, D. P. Self-powered ultrafast visible-blind UV detection and optical logical operation based on ZnO/GaN nanoscale p-n junctions. *Adv. Mater.* **23**, 649–653 (2011).
26 Peng, L., Hu, L. & Fang, X. Energy harvesting for nanostructured self-powered photodetectors. *Adv. Funct. Mater.* **24**, 2591–2610 (2014).
27 Smick, K., Villette, T., Boulton, M. E., Brainard, G. C., Jones, W., Karpecki, P., Melton, R., Thomas, R., Sliney, D. H. & Shechtman, D. Blue Light Hazard: New Knowledge, New Approaches to Maintaining Ocular Health, *Report of a Roundtable* 16 March (Essilor of America Inc., New York City, NY, USA, 2013).
28 Yamamoto, T. & Takimiya, K. Facile synthesis of highly π-extended heteroarenes, dinaphtho[2,3-b:2',3'-f]chalcogenopheno[3,2-b]chalcogenophenes, and their application to field-effect transistors. *J. Am. Chem. Soc.* **129**, 2224–2225 (2007).
29 Lee, K., Oh, M. S., Mun, S., Lee, K. H., Ha, T. W., Kim, J. H., Park, S. H., Hwang, C. S., Lee, B. H., Sung, M. M. & Im, S. Interfacial trap density-of-states in pentacene- and ZnO-based thin-film transistors measured via novel photo-excited charge-collection spectroscopy. *Adv. Mater.* **22**, 3260–3265 (2010).
30 Park, J. H., Lee, H. S., Park, S., Min, S.-W., Yi, Y., Cho, C.-G., Han, J., Kim, T. W. & Im, S. Photo-stable organic thin-film transistor utilizing a new indolocarbazole derivative for image pixel and logic applications. *Adv. Funct. Mater.* **24**, 1109–1116 (2014).
31 He, Z., Zhong, C., Su, S., Xu, M., Wu, H. & Cao, Y. Enhanced power-conversion efficiency in polymer solar cells using an inverted device structure. *Nat. Photonics* **6**, 591–595 (2012).
32 Son, D. I., Kim, H. H., Hwang, D. K., Kwon, S. & Choi, W. K. Inverted CdSe–ZnS quantum dots light-emitting diode using low-work function organic material polyethylenimine ethoxylated. *J. Mater. Chem. C* **2**, 510–514 (2014).
33 Lee, J., Hwang, H., Min, S.-W., Shin, J. M., Kim, J. S., Jeon, P. J., Lee, H. S. & Im, S. Simultaneous protection of organic p- and n-channels in complementary inverter from aging and bias-stress by DNA-base guanine/Al_2O_3 double layer. *ACS Appl. Mater. Interfaces* **7**, 1765–1771 (2015).
34 Lee, J., Kim, S. S., Kim, K., Kim, J. H. & Im, S. Correlation between photoelectric and optical absorption spectra of thermally evaporated pentacene films. *Appl. Phys. Lett.* **84**, 1701 (2004).

Supplementary Information accompanies the paper on the NPG Asia Materials website (http://www.nature.com/am)